






Amnion Epithelial Cell-Derived Exosomes Restrict Lung Injury and Enhance Endogenous Lung Repair

JEAN L. TAN ^a, SIN N. LAU,^a BRYAN LEAW,^a HONG P. T. NGUYEN,^b LOIS A. SALAMONSEN,^b MOHAMED I. SAAD ^a, SIOW T. CHAN,^a DANDAN ZHU,^a MIRJA KRAUSE,^a CARLA KIM,^c WILLIAM SIEVERT,^d EUAN M. WALLACE,^{a,e} REBECCA LIM ^{a,e}

Key Words. Fetal stem cells • Lung • Progenitor cells • Tissue-specific stem cells

^aThe Ritchie Centre and ^bCentre for Reproductive Health, Hudson Institute of Medical Research, Clayton, Victoria, Australia; ^cStem Cell Program, Children's Hospital Boston, Boston, Massachusetts, USA; ^dCentre for Inflammatory Disease and ^eDepartment of Obstetrics and Gynaecology, Monash University, Clayton, Victoria, Australia

Correspondence: Rebecca Lim, Ph.D., The Ritchie Centre, Hudson Institute of Medical Research, 27-31 Wright Street, Clayton, Victoria 3168, Australia. Telephone: 61-3-85722794; e-mail: rebecca.lim@hudson.org.au

Received July 18, 2017; accepted for publication October 20, 2017; first published January 3, 2018.

<http://dx.doi.org/10.1002/sctm.17-0185>

This is an open access article under the terms of the Creative Commons Attribution-NonCommercial-NoDerivs License, which permits use and distribution in any medium, provided the original work is properly cited, the use is non-commercial and no modifications or adaptations are made.

ABSTRACT

Idiopathic pulmonary fibrosis (IPF) is characterized by chronic inflammation, severe scarring, and stem cell senescence. Stem cell-based therapies modulate inflammatory and fibrogenic pathways by release of soluble factors. Stem cell-derived extracellular vesicles should be explored as a potential therapy for IPF. Human amnion epithelial cell-derived exosomes (hAEC Exo) were isolated and compared against human lung fibroblasts exosomes. hAEC Exo were assessed as a potential therapy for lung fibrosis. Exosomes were isolated and evaluated for their protein and miRNA cargo. Direct effects of hAEC Exo on immune cell function, including macrophage polarization, phagocytosis, neutrophil myeloperoxidase activity and T cell proliferation and uptake, were measured. Their impact on immune response, histological outcomes, and bronchioalveolar stem cell (BASC) response was assessed *in vivo* following bleomycin challenge in young and aged mice. hAEC Exo carry protein cargo enriched for MAPK signaling pathways, apoptotic and developmental biology pathways and miRNA enriched for *PI3K-Akt*, *Ras*, *Hippo*, *TGFβ*, and focal adhesion pathways. hAEC Exo polarized and increased macrophage phagocytosis, reduced neutrophil myeloperoxidases, and suppressed T cell proliferation directly. Intranasal instillation of 10 μg hAEC Exo 1 day following bleomycin challenge reduced lung inflammation, while treatment at day 7 improved tissue-to-airspace ratio and reduced fibrosis. Administration of hAEC Exo coincided with the proliferation of BASC. These effects were reproducible in bleomycin-challenged aged mice. The paracrine effects of hAECs can be largely attributed to their exosomes and exploitation of hAEC Exo as a therapy for IPF should be explored further. *STEM CELLS TRANSLATIONAL MEDICINE* 2018;7:180–196

SIGNIFICANCE STATEMENT

Idiopathic pulmonary fibrosis (IPF), a condition characterized by chronic inflammation and progressive fibrosis, is thought to arise from an impaired endogenous stem/progenitor cell response. Current treatment using nintedanib and pirfenidone targets the fibrotic phase and has minimal effect in treating the disease. This prompts the need for novel therapy targeting all aspects of this disease. Soluble factors from human amnion epithelial cell are anti-inflammatory, anti-fibrotic, and pro-regenerative, making them a potential novel therapy for IPF.

INTRODUCTION

Idiopathic pulmonary fibrosis (IPF) is a chronic and progressive fibrosing interstitial pneumonia of unknown cause that results in worsening lung function [1], with a prognosis worse than many cancers [2]. Mortality rates are estimated at about 2.54 to 11.08 per 100,000 depending on country, with rates significantly higher with increasing age [1]. Lung transplantation is currently the most effective therapy, with a 50% chance survival rate 5 years post-transplantation. As a bridge to lung transplantation and for patients who are ineligible for transplantation, drugs such as nintedanib and pirfenidone have been used in an attempt to slow progression of disease [3]. Notably, these drugs

target the progression of fibrosis but neither are curative. Given the contribution of telomerase mutations resulting in premature cellular senescence in patients with familial and sporadic pulmonary fibrosis [4], there is little wonder that drugs targeting the fibrotic process alone have limited therapeutic capability and as such a multimodal approach is warranted. To this end, a regenerative approach has been suggested to address this degenerative disease [5].

Mesenchymal stem/stromal cells (MSCs) from the bone marrow [6–8], adipose tissue [9, 10], placenta [11], and umbilical cord [12, 13] have been shown to exert beneficial effects in experimental models of lung fibrosis. Clinical testing of allogeneic stem cells has thus far shown them to

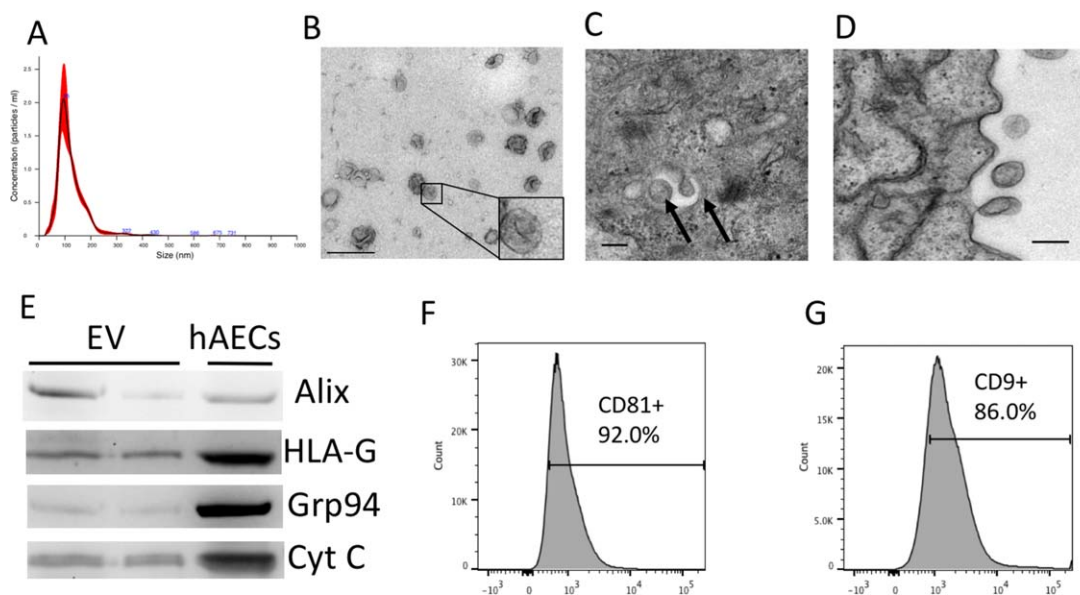


Figure 1. Characteristics of amniotic epithelial cell-derived exosomes. Nanosight analysis of exosomes show a single peak at ~ 100 nm (A). Electron microscopy showing cup-shaped morphology of exosomes, scale bar = 200 nm (B), multivesicular bodies formed within amniotic epithelial cells, scale bar = 100 nm (C), and budding of exosomes from the surface of hAEC, scale bar = 100 nm (D). Representative Western blot assessment of exosome and hAEC lysates showing presence of Alix and HLA-G in hAEC-derived exosomes and relative low abundance of Grp94 and Cyt C (E). Flow cytometry analysis of exosome show $>90\%$ positive for CD81 (F) and $>85\%$ positive for CD9 (G) markers. Abbreviations: EV, extracellular vesicles; hAEC, human amnion epithelial cell.

be safe [14, 15]; however, clinical translation of cell therapies has been fraught with technical challenges in terms of scalability and reproducibility. Alternatives such as stem cell-derived exosomes, or more broadly extracellular vesicles (EVs), are thus being concurrently pursued in applications such as myocardial infarction, pulmonary and renal fibrosis, and cutaneous wound healing [16–19].

The most well-characterized subclass of EVs to date are the exosomes, which range from 40 to 120 nm and have a flotation density of 1.13 to 1.19 g/ml [20–22]. Exosomes from MSCs were reported to have the same immunomodulatory properties as the MSCs themselves [23]. MSC-derived exosomes carrying miR-125b reportedly reduced liver fibrosis in a carbon tetrachloride model of liver fibrosis by targeting Hedgehog signaling [24]. Human amnion epithelial cells (hAEC), which have comparable properties to MSCs, can be isolated from healthy term placenta with far greater yields (hundreds of millions isolated from a single donor) [25]. This study characterized hAEC-derived exosomes and their cargo content. We also investigated the anti-inflammatory, anti-fibrotic and pro-regenerative properties of hAEC-derived exosomes in a mouse model of lung injury, specifically testing preclinical efficacy in aged mice to model the clinical setting of increasing mortality in older IPF patients.

MATERIALS AND METHODS

A complete description of the material and methods has been provided as online Supporting Information.

Human Amnion Epithelial Cell Isolation

After obtaining written informed consent, hAECs were isolated from placentae of women undergoing elective cesarean section as previously described [26] in accordance with guidelines and

approval from Monash Health Human Research Ethics Committee (#01067B). Mean gestational age of collection was $38 + 4$ weeks. EVs were isolated from 10 amnions, pooled and used for all experiments.

Human Lung Fibroblast

Exosomes from healthy human lung fibroblasts (HLF) were used controls for hAEC Exo given their previous use as control cells for comparison against hAECs [27]. HLFs were cultured under the same condition as hAECs to obtain EVs.

In Vitro Immune Potency Assays. In vitro assays to assess neutrophil, macrophage, T-cell behavior, and phenotype were performed to determine the immune potency of hAEC Exo and HLF Exo.

Mice

Animal experiments were carried out with approval by Monash University Ethics Committee and conducted in accordance with the Australian Code of Practice for the Care and Use of Animals for Scientific Purposes. C57Bl/6 mice aged 6 to 8 weeks or 12 months were housed in pathogen free Monash Medical Centre Animal facility with ad libitum access to food and water.

Bleomycin Challenge. C57Bl/6 mice received 0.04 units of bleomycin intranasally (Willow Pharmaceuticals, NSW, Australia). Each mouse was randomly allocated to receive either 10 μ g hAEC Exo or HLF Exo in 0.1 ml of saline or equal volumes of saline alone via intravenous injection. Young mice (6–8 weeks old) were treated either 24 hours (early intervention) or 7 days (late intervention) after bleomycin challenge. Aged mice (12 months old) were treated with intranasal administration of exosomes 7 days after

A

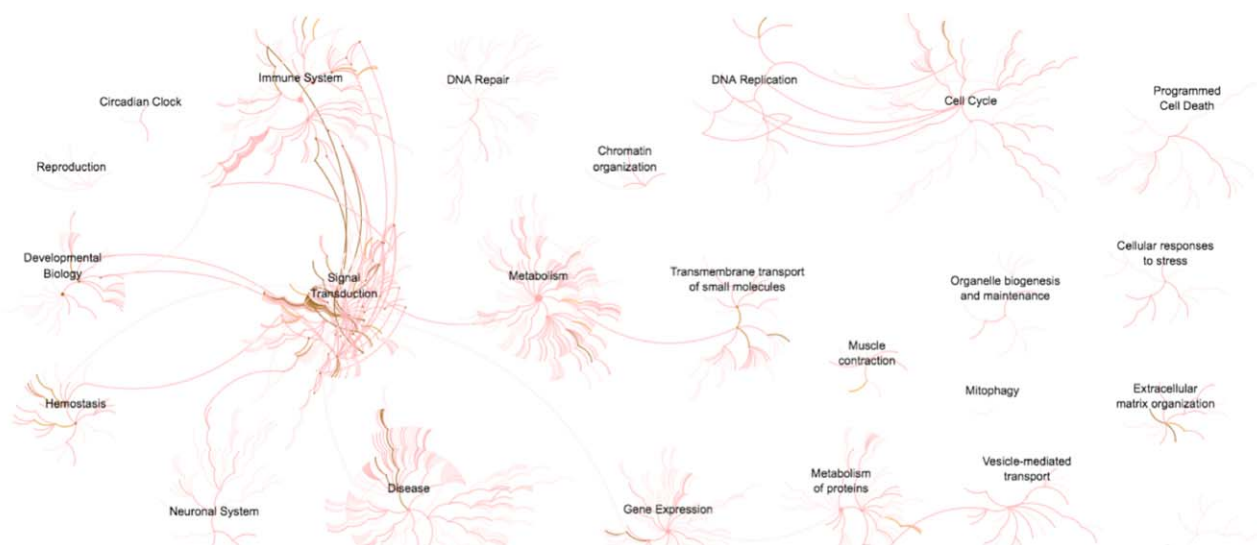


Figure 2. Proteomic and RNA seq evaluation of human amnion epithelial cell (hAEC) Exo cargo. Pathway clustering analysis showed enrichment of hAEC Exo pathways in signal transduction, immune system, developmental biology, hemostasis, neuronal system, disease, metabolism, gene expression, DNA repair, cell cycle, apoptosis, extracellular matrix organization, and as expected vesicle-mediated transport (A). Detailed pathways specific to each parent pathway mentioned above (B). Prior to sequencing, RNA quality checked using the fastQC tool and showed average quality characteristics with quality scores dropping at the end of the reads (C) and very high levels of duplication (D) and consistent distribution across most samples (E). RNA sequence analysis shows significantly overrepresented miRNA enriched in pathways for fibrosis specifically, *PI3K-Akt*, *MAPK*, *Ras*, *Hippo*, *TGF β* , and focal adhesion signaling pathways (Supporting Information Tables 2 and 3). Abbreviation: HLF, human lung fibroblasts.

bleomycin challenge. Mice were culled 7 days later. Lung tissues were collected as previously described [28]. Each group had an n of 6 to 8 per group.

RESULTS

Characterization of Extracellular Vesicles Shed by Human Amnion Epithelial Cells

There are a number of methods to isolate EV with varying purity, yield and levels of complexity. Here we show that EVs released by hAEC (hAEC-EV) can be isolated using serial ultracentrifugation with relative purity. The isolated hAEC-EV fell within the exosome size range (i.e., 80–120 nm) as determined by nanoparticle tracking analysis (Fig. 1A). Morphological assessment by transmission electron microscopy revealed a typical cup-shaped morphology (Fig. 1B). Ultrathin sections of embedded hAEC showed evidence of intracellular multivesicular bodies (Fig. 1C) and the budding of vesicles from the cell surface (Fig. 1D). Using a combination of Western blotting and bead-based flow cytometry, we observed the presence of Alix, CD81, and CD9 as well as HLA-G, a protein that is highly abundant in hAECs, with relatively low abundance of Grp94 and Cyt C (Fig. 1E–1G). Together, these findings indicated that hAEC-EV fulfilled the minimal experimental criteria of exosomes described in the position statement by the International Society for Extracellular Vesicles [29]. The EVs derived from hAECs are hereafter referred to as hAEC-derived exosomes (hAEC Exo).

Characterization of hAEC Exo

The protein composition of exosomes isolated from conditioned media from hAECs was compared with that of exosomes isolated from HLF. Protein content was analyzed by liquid chromatography followed by mass spectrometry. The data are summarized in

Figure 2 and show proteins that are enriched in hAEC Exo compared with HLF Exo. There were 84 proteins associated with the Reactome pathway by hAEC Exo, which are significantly different from HLF Exo with significance shown in Supporting Information Table 1. Proteins in hAEC Exo cargo were enriched for pathways associated with apoptosis, developmental growth, MAP kinase, inflammation mediated pathway, EGF, PDGF, and FGF signaling compared with HLF Exo cargo where pathways were centered around pathways associated with fibrosis.

A priori analysis of gene union enrichment showed overrepresentation of some miRNAs in the cargo of hAEC Exo (Supporting Information Table 2). When significantly overrepresented pathways were ranked according to the numbers of genes targeted, we noted enrichment in a number of signaling pathways associated with fibrosis. These included the *PI3K-Akt*, *MAPK*, *Ras*, *Hippo*, *TGF β* , and focal adhesion signaling pathways. A posteriori analysis of pathways union identified a dozen pathways significantly targeted by the miRNA in hAEC Exo. We observed that 110 genes associated with the KEGG pathway ‘proteoglycans in cancer’ were predicted targets of the known miRNA cargo, followed by similarly large numbers of predicted gene targets associated with *Hippo* signaling and stem cell pluripotency (Supporting Information Table 3). Additionally, reportedly anti-fibrotic microRNAs including miR-23a, miR-203a, miR-150, and miR-194 were packaged in hAEC Exo cargo.

Immunomodulatory Properties of hAEC Exo

Given previous reports on the beneficial effects of hAEC-mediated immunomodulation, we assessed the potency of hAEC Exo on a number of immune cell subsets where HLF Exo were used for comparison. Neutrophils are the first line of defense at the onset of inflammation where they oxidize tissue debris and pathogens

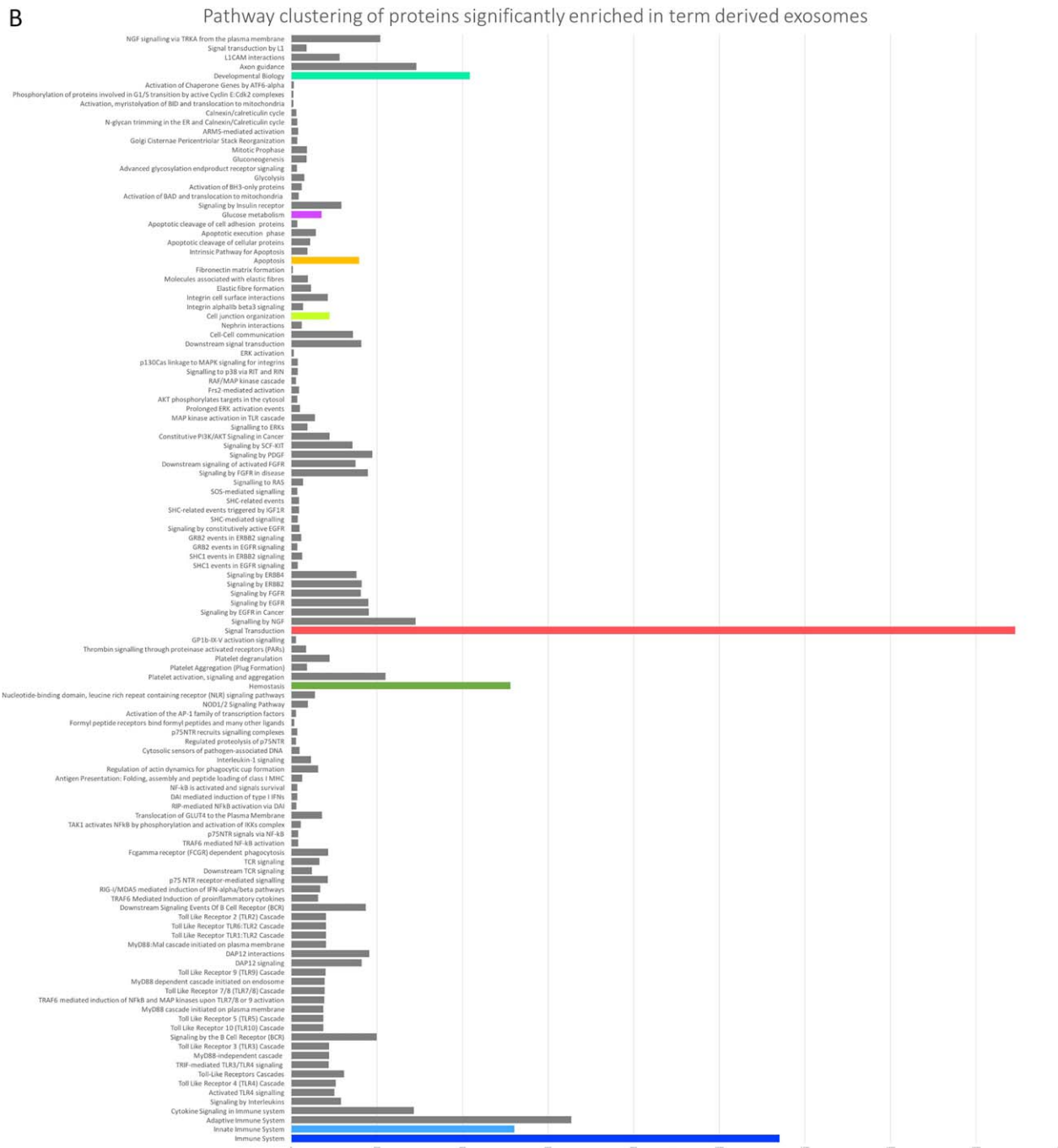


Figure 2. Continued

through myeloperoxidases (MPO) then apoptose resulting in the release of inflammatory signals to propagate downstream inflammatory responses. Here, we showed that neutrophils treated with either 1 μg or 5 μg of hAEC Exo (1 μg; $p = .022$ and 5 μg; $p = .042$, respectively, Fig. 3A) and HLF Exo (1 μg; $p = .003$ and 5 μg; $p = .012$, Fig. 3A) showed significantly lower myeloperoxidase activity than controls. Neutrophil cell death induced by hAEC Exo (1 μg; $p = .006$, 5 μg; $p = .003$, Fig. 3B) and HLF Exo (1 μg; $p = .002$, 5 μg; $p = .001$, Fig. 3B) was also higher than controls.

Correspondingly, inhibiting exosome production by incubating hAECs with 20 μM of GW4869, reversed inhibition of neutrophil MPO production by hAECs. Neutrophil cell death with GW4869 primed hAECs was 6.660 ± 0.433 significantly higher than hAECs alone (4.943 ± 0.315 , $p = .022$, Fig. 3D). However, these effects were similar in comparison to HLF Exo treatment. Next, we targeted the proceeding step in resolution where polarization of inflammatory (M1) macrophages to an anti-inflammatory (M2) state coupled with increased phagocytic clearance of apoptotic

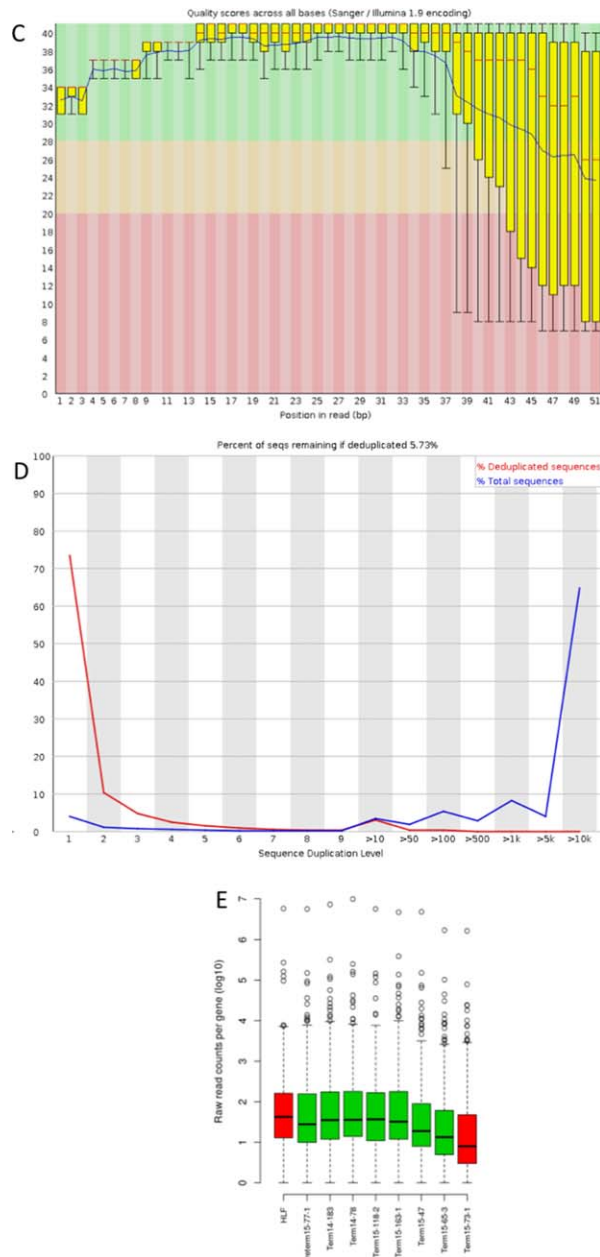


Figure 2. Continued

neutrophils are required to rid the microenvironment of further inflammatory stresses. We analyzed the effects of hAEC Exo on macrophage function and phenotype and report that 5 μ g hAEC Exo doubled the phagocytic activity of macrophages ($p = .00003$, Fig. 3E, 3F) which was not achieved by the same amount of HLF Exo. Blocking hAEC Exo release also ameliorated this effect (Fig. 3G), however with a significant increase in cell death with 20 μ M of GW4869. At 10 μ M of GW4869 hAEC-mediated increase in macrophage phagocytosis was reversed without affecting macrophage survival (Fig. 3H, 3I). Similarly, the percentage of CD206⁺ (M2) macrophages was significantly higher following stimulation with 5 μ g hAEC Exo than HLF Exo ($p = .002$) and controls ($p = .002$, Fig. 3J). Conversely, the percentage of CD86⁺ (M1) macrophages was lower with 5 μ g of hAEC Exo compared with HLF Exo and controls (Fig. 3J, $p < .0001$ and $p = .002$, respectively).

Finally, we evaluated the effect of hAEC Exo on T cell proliferation in response to CD3/CD28 stimulus and showed significant suppression of T cell proliferation index with 5 μ g of hAEC Exo at 0.400 ± 0.245 in comparison to HLF Exo (1.087 ± 0.038 , $p = .002$) and controls (1.090 ± 0.020 , $p = .002$, Fig. 3K). This effect was dependent on hAEC Exo, since blocking exosomal release using GW4869 ameliorated hAEC Exo mediated T cell suppressive effects (Fig. 3L). Next, we assessed Treg induction in CD4⁺ T cells in the context of hAEC Exo uptake in vitro. We labeled exosomal RNA and showed using Foxp3-GFP knockin CD4⁺ T cells that hAEC Exo uptake corresponded with the maturation of recipient CD4⁺ T cell into FoxP3-expressing Tregs (Fig. 3M). Inserts show colocalization of Foxp3-GFP expressing cells in green and hAEC Exo stained with exo-red dye (Fig. 3M). A video of this can be found in the Supporting Information section. These in vitro studies indicate that hAEC Exo are able to directly regulate neutrophil, macrophage, and T cell function and behavior.

hAEC Exo Prevent Bleomycin Induced Lung Injury in Young Mice

We assessed the impact of hAEC Exo in a bleomycin model of lung fibrosis when administered at Day 1 (early) and Day 7 (late) following bleomycin challenge. Given previous reports that the immune response impacts regeneration of lung tissue, we assessed hAEC Exo administration at Day 1 its impact on the immune response, bronchioalveolar stem cells (BASCs), and endothelial cells (MECs). Specifically, migration of CD11b⁺ myeloid cells during injury is shown to aid lung regeneration, and mice lacking the CD11b/CD18 heterodimer have impaired leukocyte trafficking following partial pneumonectomy and have poor lung growth [30]. In our study, we first assessed the impact of early hAEC Exo administration on inflammation as lavage fluid from IPF patients show an accumulation of neutrophils, monocytes, and T cells. Immunomodulatory effects were measured at day 7 where early intervention resulted in the reduction of CD4⁺ T cells ($p = .0140$, Table 1) and neutrophils ($p = .0018$, Table 1) in the spleen, concurrently reducing the percentage of CD4⁺ T cells ($p = .0265$, Table 1), and interstitial macrophages ($p = .062$, Table 1) in the lung. Next, we evaluated the role of hAEC Exo early intervention on transcriptional changes in BASCs and MECs. Early administration of hAEC Exo also increased expression of canonical Wnt targets; β -catenin ($p = .0082$, Fig. 4B), *BMP4* ($p = .018$, Fig. 4B), *BMPR1a* ($p = .024$, Fig. 4B), and *NFATC1* ($p = .046$, Fig. 4B) in comparison to bleomycin injured mice. Interestingly, *c-MYC* transcription was significantly reduced in BASCs from mice given hAEC Exo in comparison to bleomycin controls ($p = .041$, Fig. 4B), while *Axin1* and *Axin2* (both $p = .028$, Fig. 4D) were significantly elevated in MECs following administration of hAEC Exo compared with bleomycin controls, thus pointing to an inhibitory effect for Wnt/ β -catenin signaling in MECs. In addition to Wnt target genes, growth factor *FGFR1* was significantly elevated following hAEC Exo administration in comparison to bleomycin controls ($p = .002$, Fig. 4D). No significant differences in *CNN1D1*, *FOXM1*, *LEF1*, *PGK1*, *PTN*, *Sca1*, *TGF β* , and *WLS* transcription were seen.

hAEC Exo Resolve Bleomycin Induced Lung Injury in Young Mice

We then evaluated the effect of hAEC Exo administration on ongoing lung injury by administering the hAEC Exo 7 days after

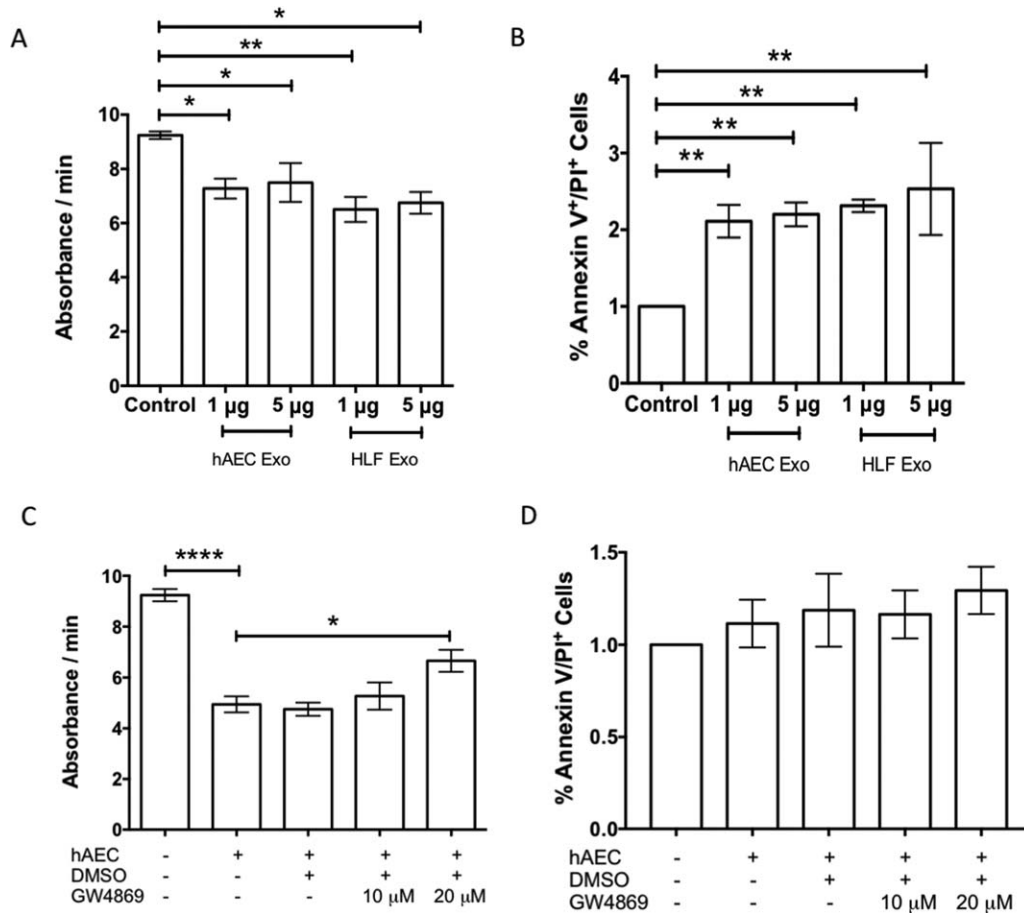


Figure 3. Immunomodulatory potency of amnion epithelial cell-derived exosomes. Neutrophil myeloperoxidase (MPO) production was significantly reduced in the presence of both hAEC [1 µg; $p = .022$ and 5 µg; $p = .042$ respectively, (A)] and HLF exosomes [1 µg; $p = .012$, (A)]. Exosomes from hAECs and HLF increases percentage of Annexin V/PI positive cells indicative of increased cell death [1 µg; $p = .006$, 5 µg; $p = .003$, (B)]. Inhibition of exosomal release by GW4869 compound reverse inhibition of neutrophil MPO activity (C) but not survival of neutrophils [GW4869 primed hAECs; 6.660 ± 0.433 vs. hAECs; 4.943 ± 0.315 , $p = .022$, (D)]. Exosomes at 5 µg increased macrophage phagocytic activity for pHRedo labeled bacterial particles [$p = .00003$, (E)]. Representative flow cytometry gating strategy of pHRedo positive macrophages pre-gated for live-dead, F4-80 and CD11b [$p = .00003$, (F)]. GW4869 neutralized hAEC Exo mediated increase in macrophage phagocytosis (G). Percentage of live:dead macrophages was unchanged in the presence of hAEC and HLF exosomes (H). Addition of 20 µM of GW4869 and equal volumes of DMSO increased macrophage cell death (I). Macrophage polarization was skewed toward M2 CD206+ phenotype and away from M1 CD86+ phenotype with increasing dose of hAEC exosomes [$p < .0001$ and $p = .002$ respectively, (J)]. T cell proliferation was significantly suppressed with 5 µg of hAEC exosomes [5 µg; 0.400 ± 0.245 vs. control; 1.090 ± 0.020 , $p = .002$, (K)]. Addition of GW4869 reversed this effect but was not significant (L). Representative images of control (Exo-Red label only) against Exo-Red labeled hAEC Exo uptake by GFP-Foxp3 CD4⁺ T cells with red arrows pointing uptake of RNA exosome labeled in red by transgenic GFP-Foxp3 CD4 T cells (M). Only red signals of high abundance are labeled with red arrows. Green arrows point to GFP-Foxp3 positive cells. Colocalization of green and red are represented by both arrows. A video of hAEC Exo uptake can be found on Supporting Information data. (*, $p < .05$; **, $p < .01$; ***, $p < .001$). Abbreviations: hAEC Exo, human amnion epithelial cell-derived exosomes; HLF exo, HLF exosomes; DMSO, dimethyl sulfoxide.

bleomycin challenge (late intervention). Histological outcomes of inflammation, fibrosis, and progenitor cell counts were measured at day 14. The percentage of tissue-to-airspace ratio was improved ($p \leq .001$, Fig. 4E); lung collagen content and α SMA expression were significantly lower ($p \leq .01$, Fig. 4F, $p = .176$, Fig. 4G). Additionally, the average number of BASCs per terminal bronchiole was significantly higher in hAEC Exo than bleomycin controls ($p = .017$, Fig. 4I), and hAEC Exo increased the percentage of ATII, another endogenous lung progenitor cell subtype ($p = .018$, Fig. 4J), while ATI remained unchanged (Fig. 4K). Next, we evaluated the gene expression of sorted BASCs and MECs and found that fewer genes were affected by late intervention compared with early intervention in both cell population. In the late intervention group, hAEC Exo did not alter gene expression of BASCs in comparison to bleomycin controls but significantly increased MEC expression of *FZD6*

($p = .0287$, Fig. 4P) and *GATA6* ($p = .0288$, Fig. 4P) compared with bleomycin controls. These findings show that hAEC Exo given at different phases of lung injury can attenuate inflammation and alter transcriptional changes in BASCs and MECs.

hAEC Exo Prevent Bleomycin Induced Lung Injury in Aged Mice

Pulmonary fibrosis is a disease affecting the aged population who are predisposed to mutations in telomerase resulting in telomere shortening and potential loss of regenerative capacity. Accordingly, we evaluated the effects of delayed hAEC Exo administration in aged mice with established pulmonary fibrosis. In our hands, hAEC Exo administration ameliorated lung fibrosis in aged mice compared with bleomycin and HLF Exo controls. Specifically, there was no evidence of bronchoalveolar hyperplasia in hAEC Exo

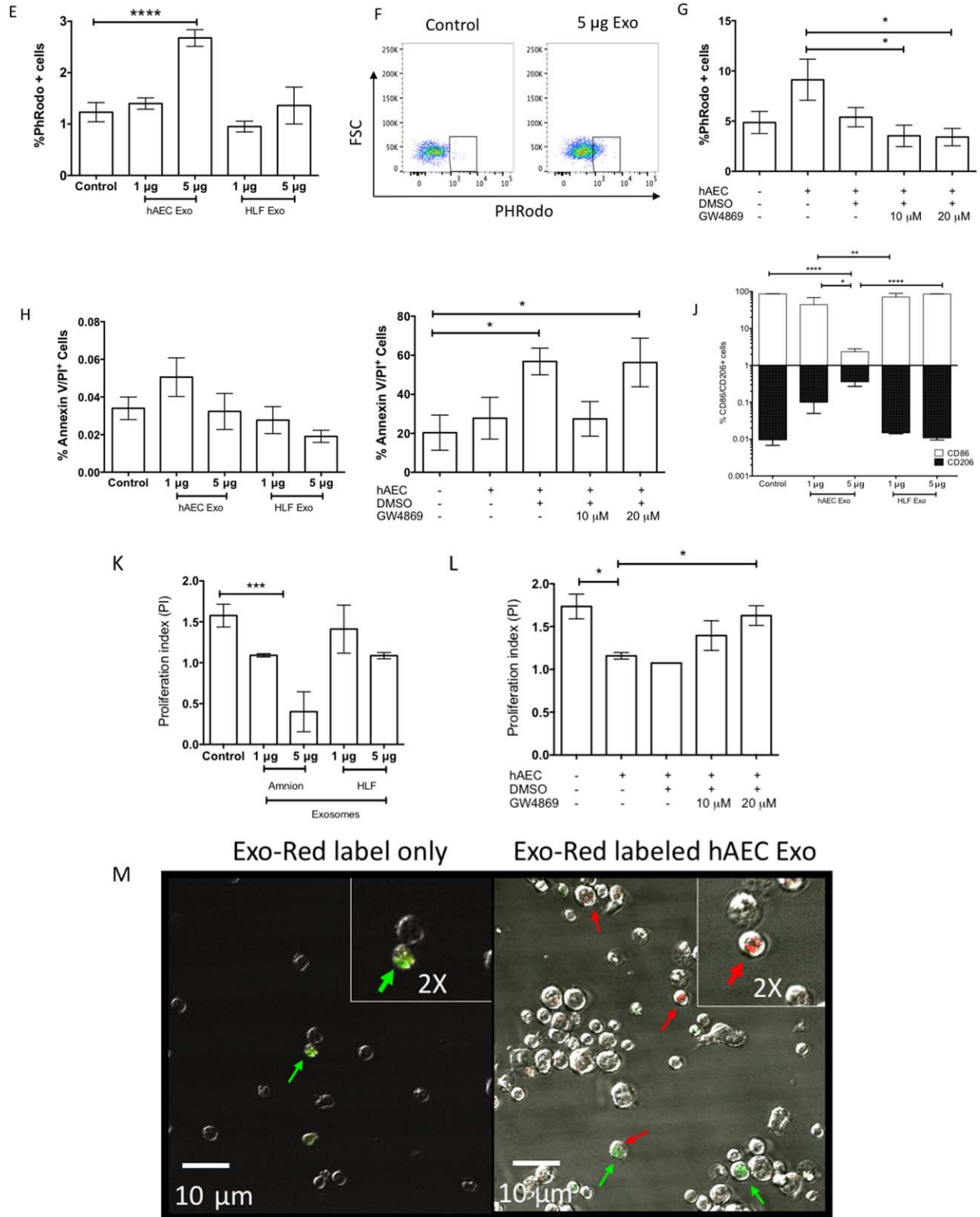


Figure 3. Continued

treated aged mice and an approximate twofold reduction in pulmonary collagen ($p \leq .01$, Fig. 5A) and depletion of α -SMA+ cells compared with bleomycin controls ($p \leq .05$, Fig. 5B). The average number of BASCs per terminal bronchiole was higher in hAEC Exo

groups than bleomycin controls ($p = .036$, Fig. 5E). The mean percentage of alveolar type II (SPC^+CC10^+) and type I ($Pdnp^+$) cells were also higher in the hAEC Exo group compared with bleomycin controls (ATII; $p = .02$, ATI; $p = .02$, Fig. 5F, 5G).

Table 1. Immune cell phenotyping at day 7

	Spleen				Lung			
	Saline vehicle	Bleomycin saline	Bleomycin 10 µg hAEC EV	Bleomycin 10 µg HLF EV	Saline vehicle	Bleomycin saline	Bleomycin 10 µg hAEC EV	Bleomycin 10 µg HLF EV
CD4⁺	11.118 ± 1.395	11.804 ± 2.316	8.06 ± 1.487	10.664 ± 1.896	4.646 ± 0.287	7.358 ± 1.536	8.476 ± 2.162	4.922 ± 0.763
CD4⁺CD3⁺	9.524 ± 1.364	9.918 ± 2.116	6.378 ± 1.182	9.006 ± 1.518	3.962 ± 0.151	4.324 ± 0.458	4.958 ± 0.570	3.892 ± 0.457
CD4⁺CD3⁺CD25⁺	0.01464 ± 0.0124	0.04468 ± 0.012	0.66 ± 0.086	0.726 ± 0.099	0.01464 ± 0.012	0.04468 ± 0.012	0.66 ± 0.086	0.726 ± 0.099
Foxp3⁺Tregs	0.00304 ± 0.002	0.01776 ± 0.004	0.036 ± 0.010	0.0342 ± 0.006	ND	0.00016 ± 0.0001	0.00016 ± 0.0001	0.00016 ± 0.0001
CD8⁺	6.95 ± 1.042	7.97 ± 1.762	4.132 ± 0.979	5.838 ± 1.387	3.44 ± 0.151	3.0325 ± 0.529	3.262 ± 0.273	9.156 ± 3.266
CD8⁺CD3⁺	4.996 ± 1.098	5.748 ± 1.397	3.028 ± 0.623	4.216 ± 0.945	0.0544 ± 0.007	1.3926 ± 0.850	0.0238 ± 0.002	0.0848 ± 0.043
CD4⁺CD8⁺CD3⁺	0.44 ± 0.0365	0.536 ± 0.124	0.672 ± 0.087	1.066 ± 0.134	0.392 ± 0.051	0.1058 ± 0.043	0.23 ± 0.0624	0.276 ± 0.063
CD4⁺CD8⁺CD3⁺Foxp3⁺	0.00088 ± 0.001	0.00472 ± 0.001	0.04956 ± 0.020	0.08 ± 0.015	0.00072 ± 0.001	0.00272 ± 0.002	0.00016 ± 0.0001	0.00024 ± 0.0002
Neutrophils	0.00704 ± 0.003	0.00408 ± 0.002	0.0116 ± 0.002 *	0.01836 ± 0.005	0.0232 ± 0.005	0.0256 ± 0.0054.	0.0324 ± 0.0063	0.01932 ± 0.0064
Interstitial macs	0.00032 ± 0.00032	0.0004 ± 0.0002	0.00016 ± 0.00001	ND	0.086 ± 0.0213	0.3392 ± 0.1648	0.2684 ± 0.1034	0.1972 ± 0.077
CD103 DCs	ND	ND	ND	ND	0.003888 ± 0.0016	0.00876 ± 0.0033	0.0014198 ± 0.0005	0.001187 ± 0.0006
CD11b DCs	0.00016 ± 0.00001	ND	0.00024 ± 0.00024	0.00016 ± 0.00001	0.01648 ± 0.0052	0.01824 ± 0.0072	0.0268 ± 0.0052	0.021 ± 0.0026

Abbreviations: hAEC EV, human amnion epithelial cell extracellular vesicle; HLF EV, human lung fibroblasts extracellular vesicle.

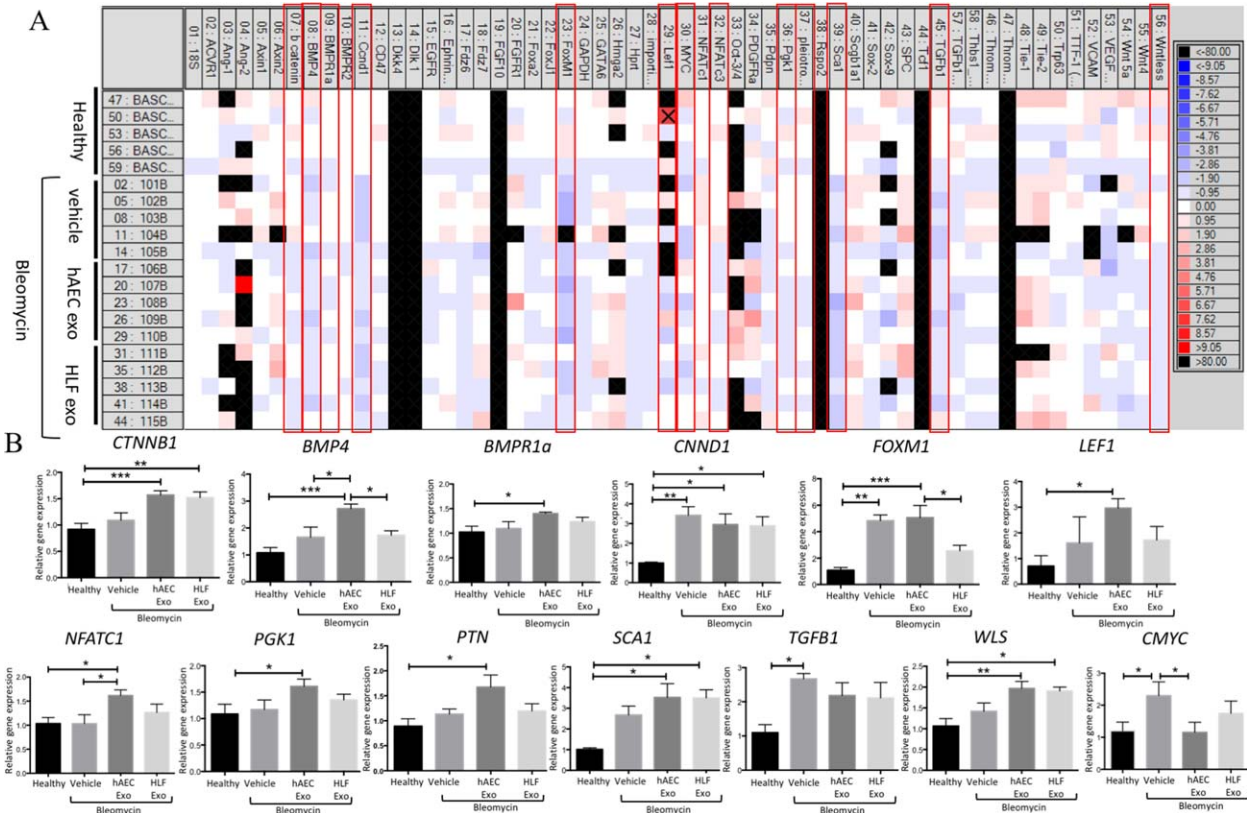


Figure 4. Early intervention in young mice. Exosomes given at Day 1 significantly reduced CD4⁺, CD3 + CD4⁺, and CD8⁺ T cell splenocytes but only reduced lung CD4⁺ T cells (Table 1). Exosomes from HLF and hAECs similarly reduced neutrophil and interstitial macrophage percentages in spleen and lung respectively (Table 1). Representative heat map of genes expressed by BASCs sorted from healthy, bleomycin, bleomycin + hAEC exo, and bleomycin + HLF exo mice (A). Quantitative PCR analysis on sorted BASCs showed increase in *CTNNB1*, *BMP4*, *FOXM1*, *LEF1*, *NFATC1*, *PGK1*, *PTN*, *SCA1*, and *WLS* with a reduction of *cMYC* gene expression (B). Representative heat map of genes expressed by mouse endothelial cells (MECs) sorted from healthy, bleomycin, bleomycin + hAEC exo, and bleomycin + HLF exo mice (C). Sorted MECs showed increased *Ang2*, *Axin1*, *Axin2*, *BMPR2*, *EFNB2*, *FGFR1*, *LEF1*, *NFATC3*, and *THBS1* gene expression (D). Day 7 hAEC exo intervention on fibrotic lung injury in young mice. Exosomes given 7 days after bleomycin challenge then culled at day 14 showed significant reduction in inflammation; H&E stain, collagen content; Sirius red and α -SMA staining [$p \leq .001$, (E), $p \leq .01$, (F), $p = .176$, (G)]. Representative histological staining for H&E, Sirius red, and α -SMA [scale bar = 50 μ m, (H)]. Average bronchoalveolar stem cell (BASC) counts per terminal bronchiol increased with hAEC Exo intervention [$p = .017$, (I)]. Average ATI counts increased with hAEC intervention [$p = .018$, (J)]. No changes were seen in ATI cells (K). Representative image of BASCs stained with CC10 in green, ATI cells stained with SPC in red and CC10, ATI cells, stained with Pdpn in white over nuclear DAPI stain in blue [scale bar = 50 μ m, (L)]. Representative heat map of genes expressed by BASCs sorted from healthy, bleomycin, bleomycin + hAEC Exo, and bleomycin + HLF Exo mice (M). Exosomes given 7 days post bleomycin significantly increased *BMP4* and *CNN1D1* gene expression in BASCs (N). Representative heat map of genes expressed by MECs sorted from healthy, bleomycin + hAEC exo and bleomycin + HLF exo mice (O). Exosomes given 7 days post bleomycin increased *FZD6* and *GATA6*, gene expression in MECs [*FZD6*; $p = .0287$, *GATA6*; $p = .0288$ (P)]. (*, $p < .05$; **, $p < .01$; ***, $p < .001$). Abbreviations: BASCs, bronchioalveolar stem cells; hAEC Exo, human amnion epithelial cell-derived exosomes; HLF exo, HLF exosomes.

Pro-Regenerative Properties of hAEC Exo

Current evidence suggests that in IPF, an imbalance in cell signaling leads to alveolar epithelial senescence and over activation of myofibroblast. Hence, our next step was to assess the regenerative and anti-fibrotic ability of hAEC Exo in culture. To address this, we assessed the direct effects of hAEC Exo on BASC growth and fibroblast activation. BASCs from healthy mice cultured with hAEC Exo formed differentiated lung cells including alveolar, bronchiolar, and bronchioalveolar colonies after 21 days in culture (Fig. 6A). The addition of hAEC Exo resulted in more bronchiolar colonies and colonies were larger compared with those cultured in media alone ($p < .0001$, Fig. 6B and $p < .0001$, Fig. 6C). Number of alveolar colonies per well and area covered per alveolar colony were also higher in hAEC Exo treated BASCs than control media ($p = .003$, Fig. 6D; $p = .0001$, Fig. 6E). The expression of club cell marker (CC10) was higher in bronchiolar

colonies treated with 5 μ g ($p = .001$, Fig. 6Fi) and 10 μ g ($p = .00028$, Fig. 6Fii) hAEC Exo compared with media alone. Additionally, mixed colonies increased expression of ciliogenesis marker Foxj1 following culture with hAEC Exo at 5 μ g ($p = .033$, Fig. 6Fiii) and 10 μ g ($p = .030$, Fig. 6Fiii).

To assess the direct effects of hAEC Exo on myofibroblast differentiation, HLF were cultured in the presence of *TGF β* and exposed to either hAEC Exo or pirfenidone. The impact of hAEC Exo on myofibroblast differentiation was dose dependent. At 24 hours, suppression of fibroblast activity was greater with 5 μ g of hAEC Exo compared with 1 μ g and control media, which was comparable to the inhibitory effects of 0.2 mM of pirfenidone ($p = .003$, $p = .040$, respectively, Fig. 6H). A similar trend in collagen production was measured where at 5 μ g of hAEC Exo was better at reducing HLF collagen deposition compared with 0.2 mM of pirfenidone ($p = .887$, Fig. 6I).

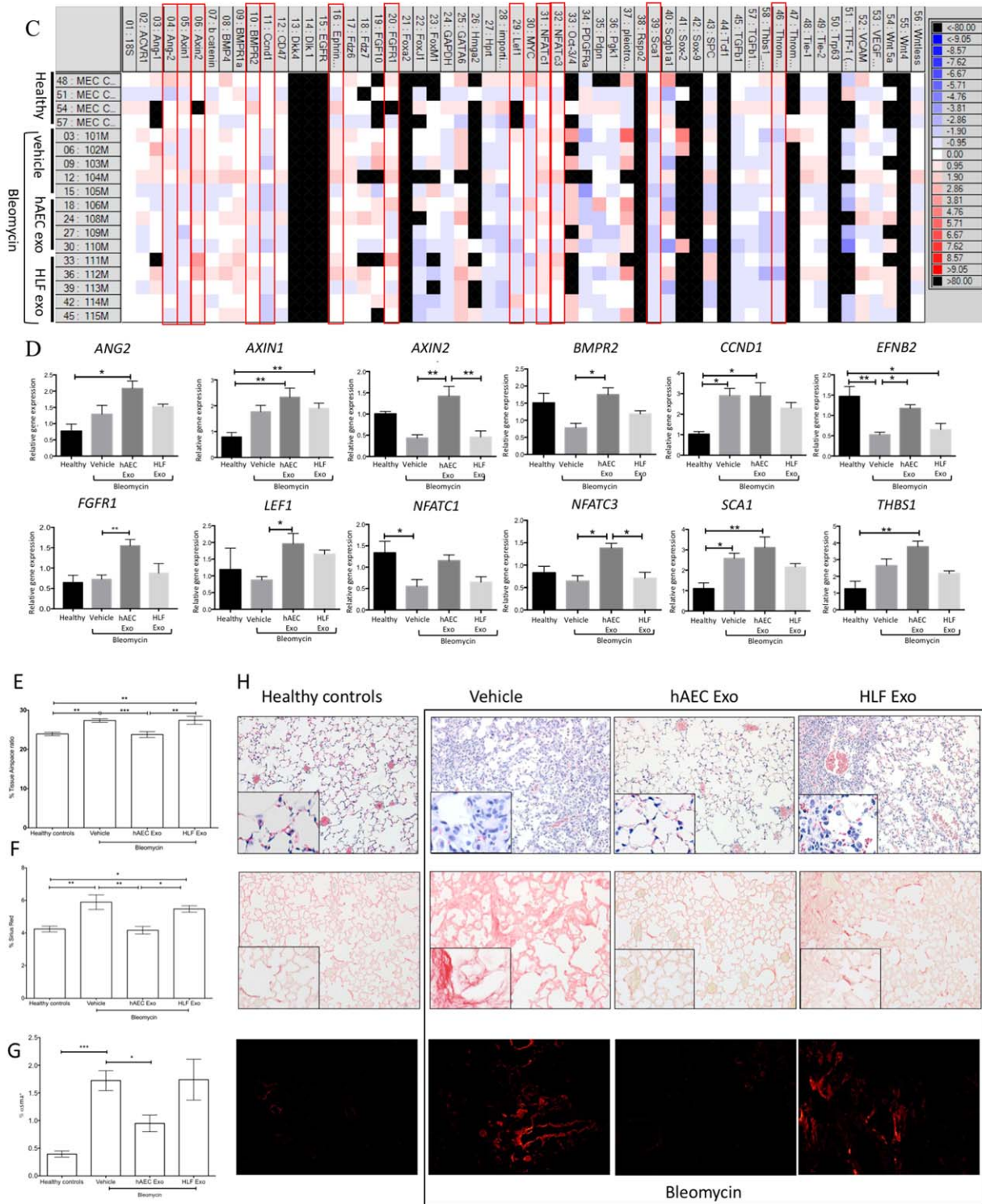


Figure 4. Continued

DISCUSSION

Lung transplantation remains the only effective therapy for IPF. Current preclinical studies using cell-based therapies to treat lung fibrosis have yielded mixed results between cell types. In particular, studies using MSCs, when given 7 to 14 days after bleomycin regardless of its source, have shown varying outcomes in

amelioration of fibrosis. Specifically, in the case of hAECs, we have shown that given 14 days post bleomycin resulted in significant amelioration of fibrosis in comparison to administration at day 7. We believe that hAECs respond to their microenvironment by releasing exosomes and the contents in hAEC Exo released in an inflammatory environment would not contain potent pro-regenerative, anti-fibrotic, and pro-inflammatory properties. To

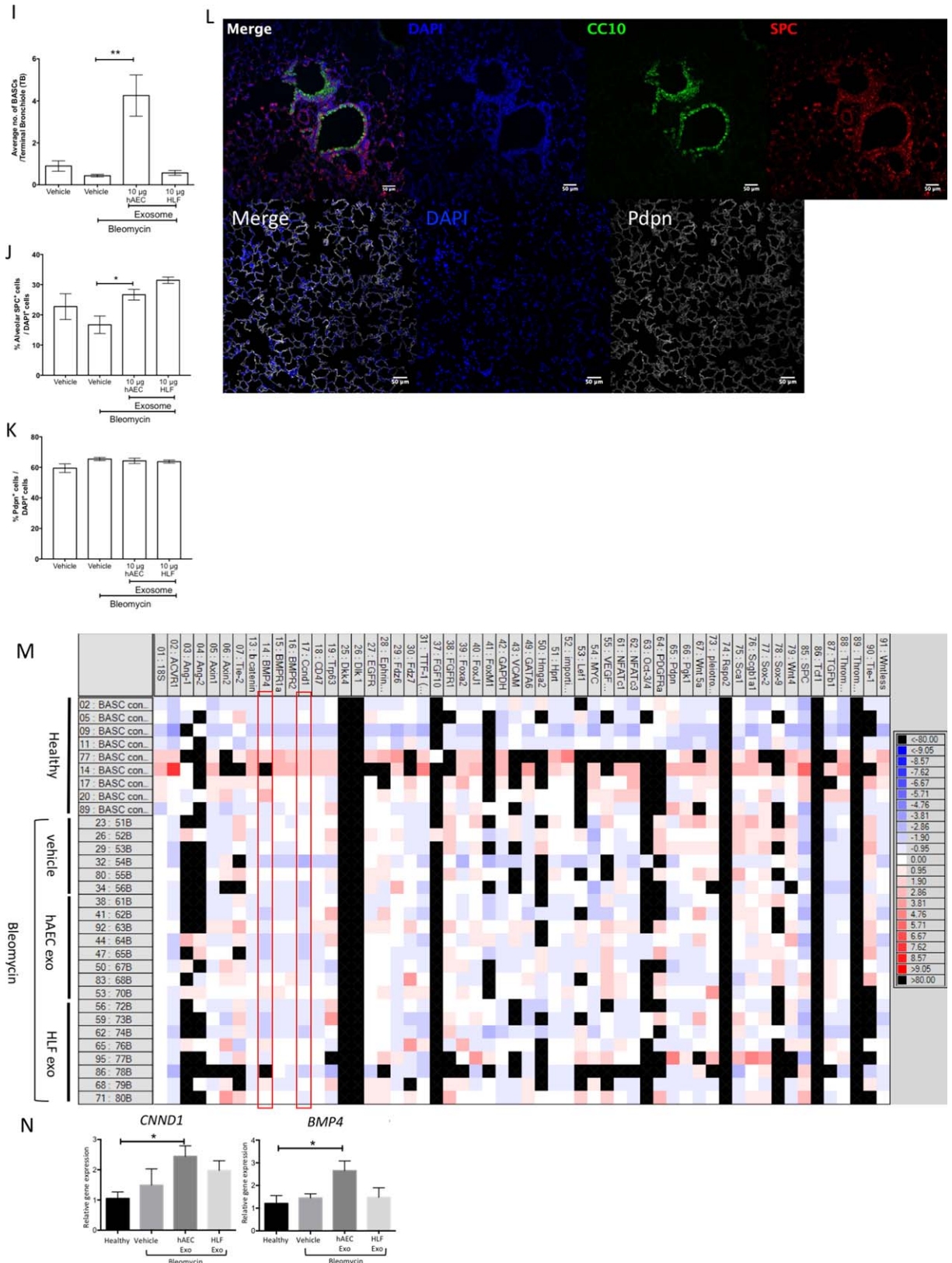


Figure 4. Continued

our knowledge, this is the first study to report that hAEC Exo treatment targets the inflammatory, fibrotic, and regenerative cascades of pulmonary fibrosis. In line with our interests in clinical

translation, we assessed the ability of hAEC Exo to prevent and reverse lung inflammation and fibrosis, and we chose a delivery method (intranasal) that would be clinically useful. Given the

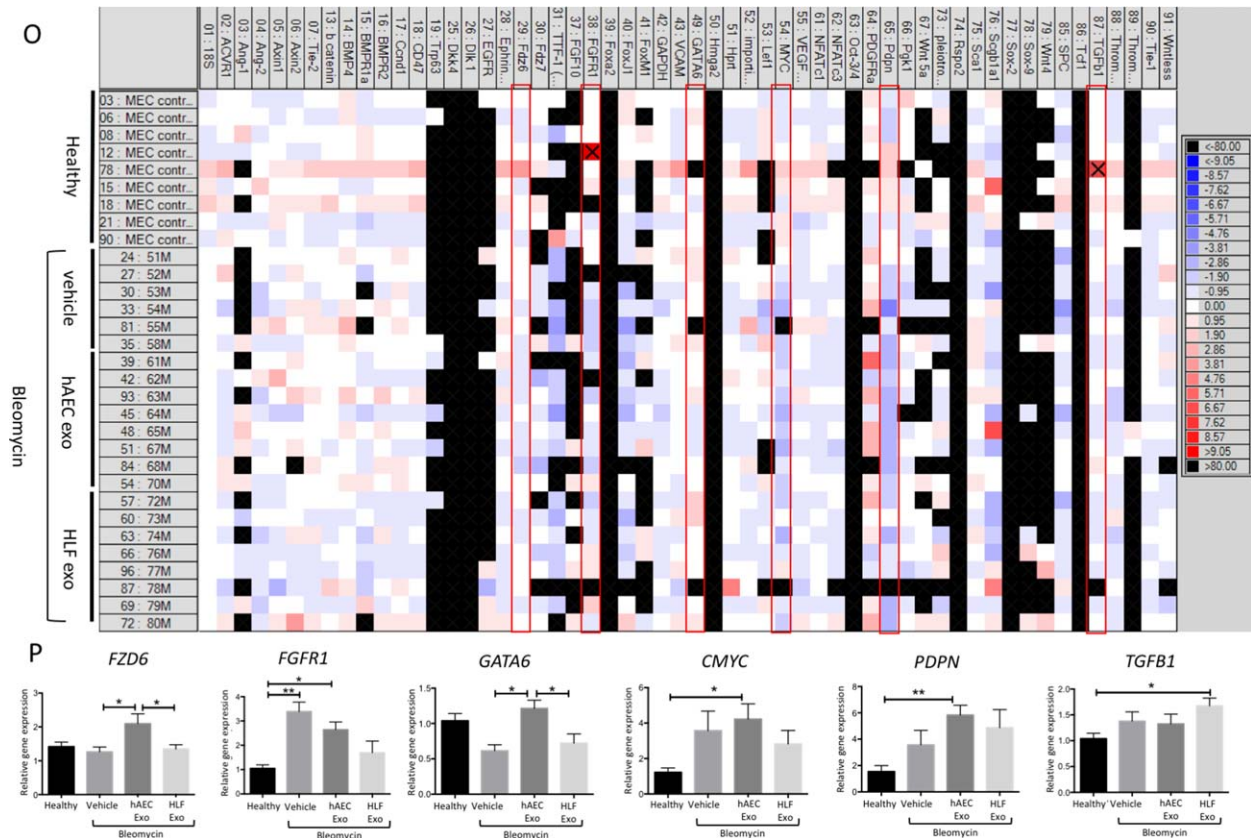


Figure 4. Continued

degenerative nature of IPF, we also sought to ascertain the impact of hAEC Exo on endogenous lung stem/progenitor cells, and in aged animals.

In response to damage, immune cells particularly neutrophils and CD4 T cells release cytokines, growth factors, and stimuli to modulate fibroblast and macrophage behavior [31]. However, an aberrant immune response contributes to the pathogenesis of IPF, and thus we first show that hAEC Exo cargo were enriched for proteins involved in immunomodulation. Specifically, we found that proteins involved in Fc-gamma receptor dependent phagocytosis and regulation of actin dynamics for phagocytic cup formation pathways were enriched in hAEC Exo. This was in line with our observations of increased macrophage phagocytic activity mediated by hAEC Exo, and supports earlier work by others showing that hAEC-conditioned media exerts similar effects [32, 33]. hAEC Exo also contained protein cargo enriched for P38 and *PI3K-Akt* pathways. P38 is critical to tissue regeneration, where p38 α deletion results in immature and hyperproliferative lung epithelium [34]. Similarly, the *PI3K-Akt* pathway is critical for cell survival, cell cycle, and macrophage polarization [35]. Next, we evaluated the immunomodulatory properties of hAEC Exo. Here, we showed that hAEC Exo at 5 μ g increased their phagocytic activity and changed their polarization state, which was possibly mediated by the *PI3K-Akt* signaling pathway [36]. Neutrophil myeloperoxidase activity was also reduced with both hAEC and HLF Exo, in conjunction with increased neutrophil apoptosis. This was particularly interesting, since HLF Exo were unable to prevent lung fibrosis in vivo despite inhibiting neutrophil activation in vitro. It is suggestive that exosomes from healthy lung fibroblast have the ability to

modulate neutrophil response. However, this effect alone is insufficient to abolish this disease and targeting more than one cascade of this disease may be fundamental [37]. Neutrophil and macrophage activity encompasses the innate inflammatory response and is accompanied by the T cell adaptive immune response. As such, we evaluated the behavior of T cells and showed that hAEC Exo can suppress CD3/CD28 activated T cell proliferation. Additionally, this suppression of T cell proliferation coincided with hAEC Exo uptake, which occurred within minutes and was sufficient for Treg activation. This is in line with previous observations that dendritic cell-derived exosomes suppressed collagen-reactive T cells through their packaging of Fas-ligands [38]. Using a mouse model of bleomycin induced lung injury, we found that early intervention with hAEC Exo significantly decreased the percentage of splenic CD4+ CD3+, CD8+ T cells, and neutrophils, with concurrent reduction of CD4+ T cells and interstitial macrophages in the lungs. These findings suggest that hAEC Exo may directly modulate the behavior and phenotype of neutrophils, macrophages, and T cells both in vitro and that in vivo outcomes may be as a consequence of their uptake by specific target cells.

Next, evaluation of hAEC Exo anti-fibrotic protein cargo revealed an enrichment of proteins associated with the PDGF, FGF, and EGF signaling pathways, which have been implicated in vascular remodeling, regulation of fibroblast proliferation and development, migration, adhesion, and cell survival, respectively. We found an overrepresentation of proteins in hAEC Exo that were involved in negatively regulating FGFR1 and FGFR2, and PDGF-mediated regulation of *RAS* through *GAPs* target pathways

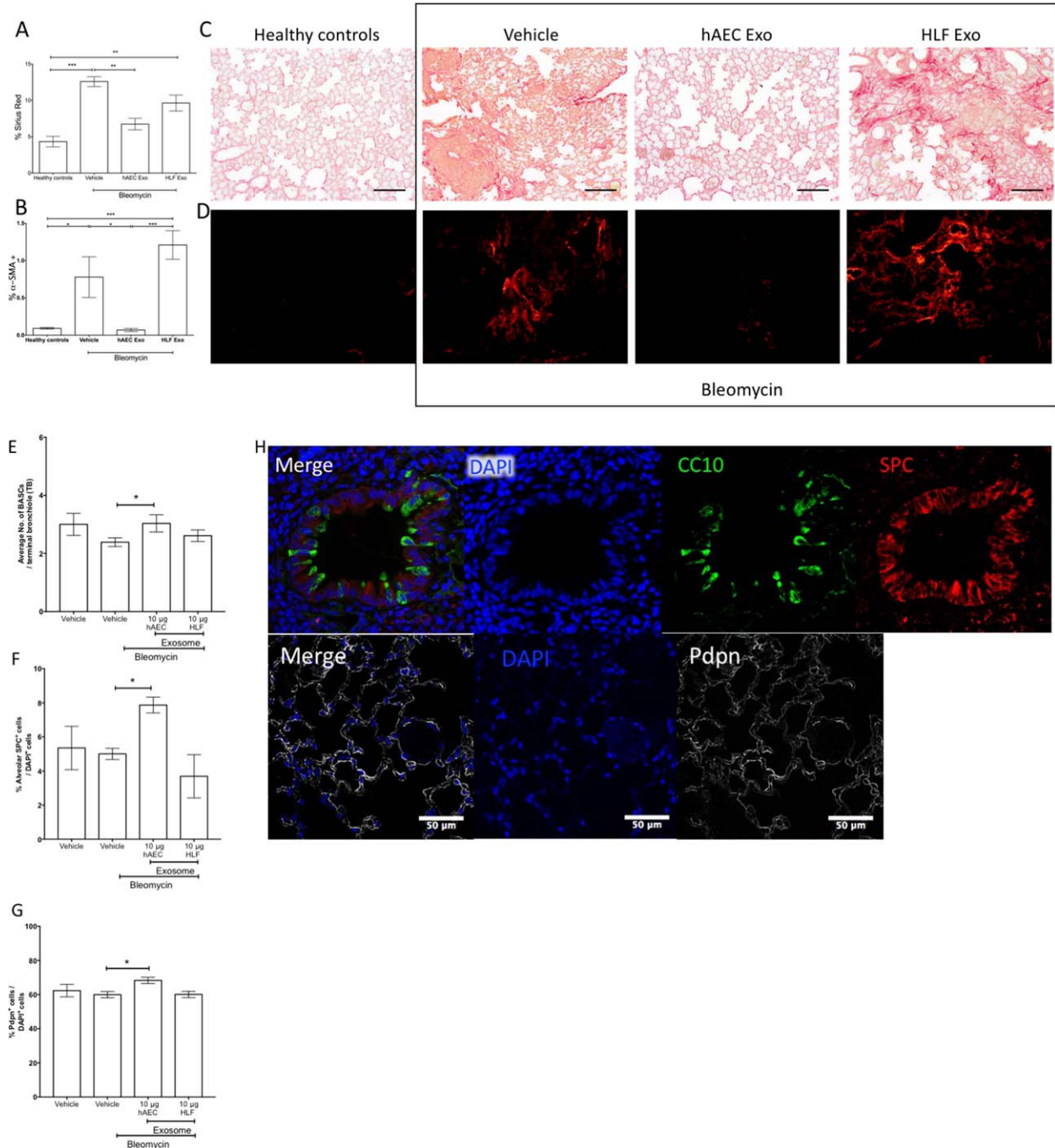


Figure 5. Late intervention in aged mice. hAEC Exo given 7 days after bleomycin challenge showed significant reduction in collagen content; Sirius red and α -SMA staining [$p \leq .01$, (A), $p \leq .05$, (B)]. Representative images of Sirius red and α -SMA staining in aged mice [scale bar = 50 μ m, (C, D)]. Average bronchioalveolar stem cell (BASC) counts per terminal bronchiole increased with hAEC Exo [$p = .0167$, (E)]. Alveolar type II and type II epithelial cell counts were higher in hAEC Exo [ATI; $p = .02$, ATI; $p = .02$, (F, G)]. Representative images of BASCs, ATI, and ATI staining [scale bar = 50 μ m, (H)]. (*, $p < .05$; **, $p < .01$; ***, $p < .001$). Abbreviations: hAEC Exo, human amnion epithelial cell-derived exosomes; HLF exo, human lung fibroblasts exosomes.

common to those targeted by nintedanib. RNA-Seq analysis showed that hAEC Exo contain miRNAs that converge on key pathways associated with fibrosis as well as cancer and stem cell pluripotency. In keeping with the apparent impact of hAEC Exo administration on lung fibrosis, we noted the presence of a number of reportedly anti-fibrotic miRNAs. Among the 10 most abundant miRNAs were miR-27a, which reportedly targets

myofibroblast differentiation, and lentiviral delivery of miR-27a-3p diminished bleomycin induced lung fibrosis [39]. hAEC Exo also packaged miRNAs that target various aspects of *TGF β* signaling including miR-23a, which inhibits Smad 2 [40], miR-203a which inhibits Smad 3 and thereby contributes to the repression of *TGF β* mediated epithelial-mesenchymal transition as well [41], and miR-34a which induces lung fibroblast senescence and suppresses

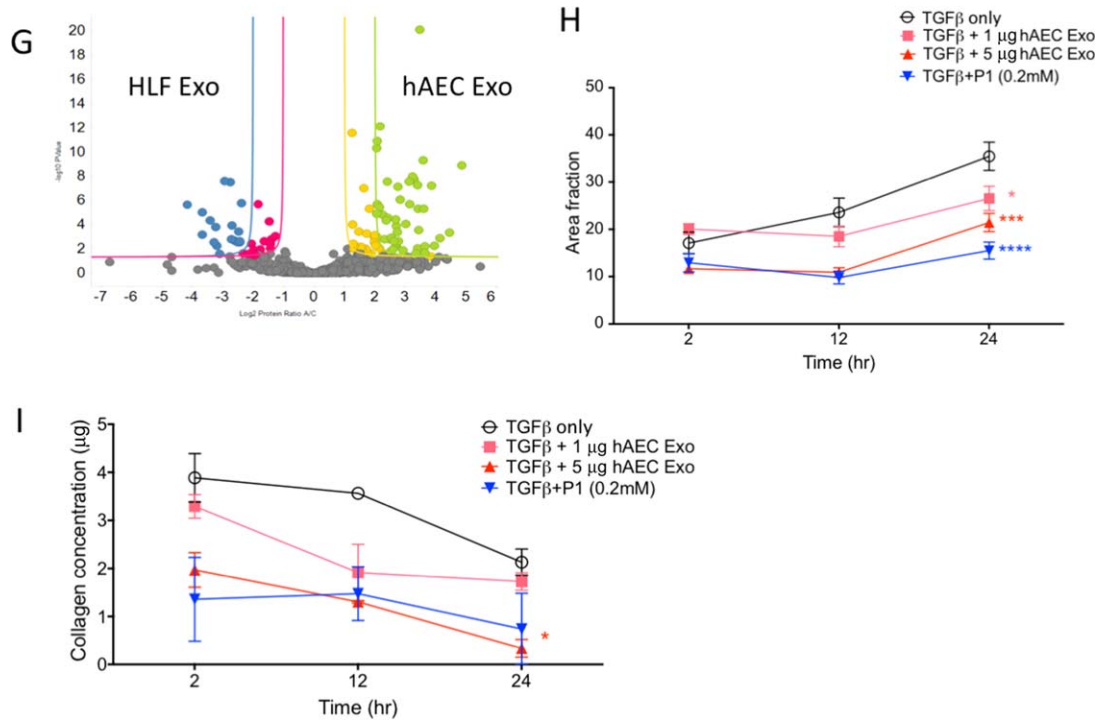


Figure 5. Continued

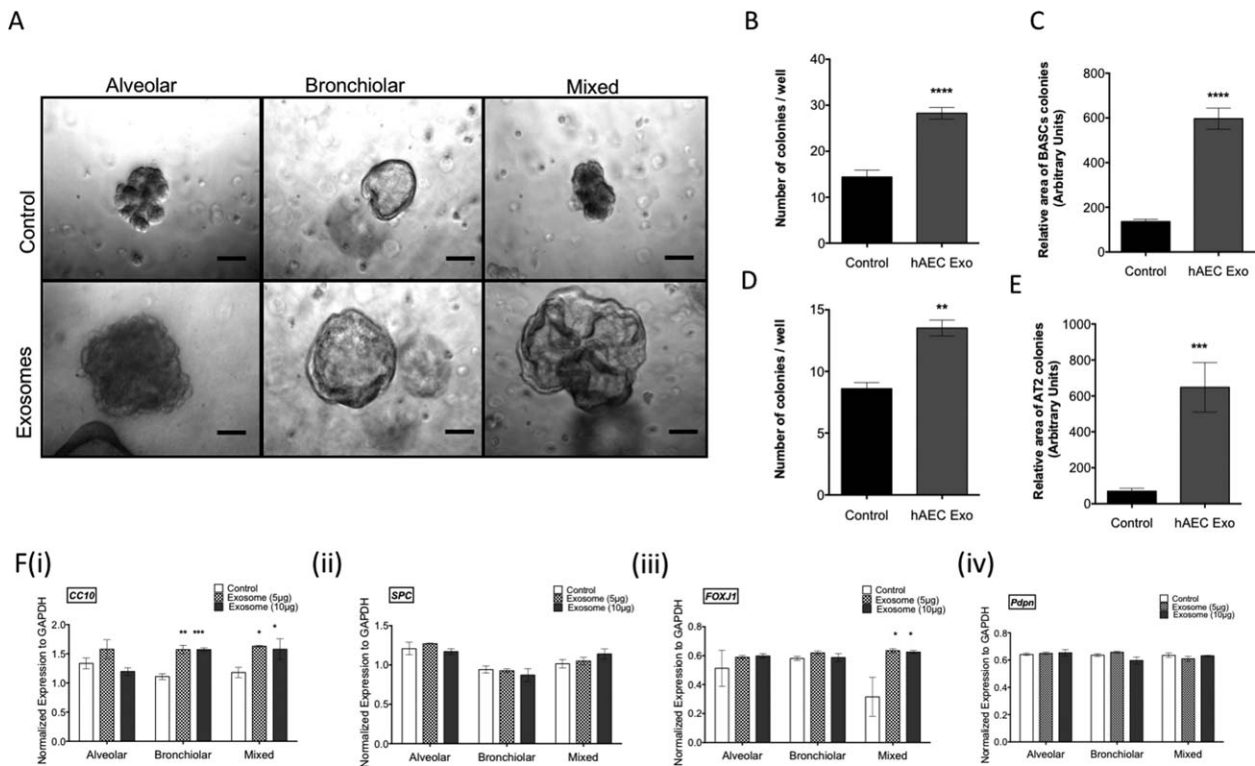


Figure 6. Regenerative potency of exosomes in vitro. BASCs sorted from healthy mice formed alveolar, bronchiolar, and bronchioalveolar organoids in culture. [scale bar = 10 μm, (A)]. Culture with hAEC Exo significantly elevated the number and relative area of BASC colonies per well [$p < .0001$, (B) and $p < .0001$, (C)]. hAEC Exo also increased the number and relative area of AT2 colonies per well [$p = .003$, (D); $p = .0001$, (E)]. Quantitative PCR analysis showed hAEC Exo significantly increased expression of *CC10* in bronchiolar and *FOXJ1* in mixed colonies [5 μg; $p = .001$, (Fi) and 10 μg; $p = .00028$, (Fii), 5 μg; $p = .033$, (Fiii), and 10 μg; $p = .030$, (Fiii)]. No changes were seen in expression of *SPC* (Fii) and *Pdpn* (Fiv). Volcano plot showing collection of proteins enriched in hAEC Exo, in green and yellow over proteins enriched in HLF Exo, in red and blue (G). Human lung fibroblasts activation by *TGFβ* measured by collagen deposition was significantly reduced when cultured with hAEC Exo at a dose dependent manner with effects closely resembling pirfenidone [5 μg; $p = .003$, 1 μg; $p = .040$, respectively, (H)]. Inhibition of HLF differentiation into myofibroblasts were inhibited by 5 μg of hAEC Exo similar to effects by pirfenidone [5 μg; $p = .887$, (I)]. (*, $p < .05$; **, $p < .01$; ***, $p < .001$). Abbreviations: BASC, bronchioalveolar stem cell; hAEC Exo, human amnion epithelial cell-derived exosomes.

fibroblast proliferation [42]. Furthermore, **miR-150** and **miR-194**, both of which are enriched in hAEC Exo, inhibit the activation of hepatic stellate cells and reduce collagen deposition in the setting of liver fibrosis by inhibiting *c-MYC* and *RAC 1* expression [43]. Future studies validating the contribution of each miRNA in the anti-fibrotic effects of hAEC Exo must be undertaken in order to ascertain their relevance and enable the development of hAEC Exo as a therapeutic for IPF. Interestingly, hAEC Exo miRNA cargo was also found to converge on the *Hippo* signaling pathway, which has been implicated in regeneration and repair. Specifically, the *Hippo* pathway regulates lung progenitor cell response and differentiation [44]. The converse role of *Hippo* signaling in cancer and indeed the convergence of miRNAs on proteoglycans in cancer should not be ignored, and the impact of hAEC Exo on tumorigenesis should be investigated further.

The significant improvement observed with the late intervention cohort is in keeping with the direct anti-fibrotic effects of hAEC Exo. We noted that hAEC Exo were able to directly suppress myofibroblast differentiation and decrease collagen production in vitro, comparable to pirfenidone. Since there is growing interest in the role of aging and telomerase mutations in the development of IPF [45, 46], we sought to assess the impact of delayed hAEC Exo in aged mice and found them to be comparably effective as they were in young mice. It is encouraging to show that hAEC Exo can abolish fibrosis and may have regenerative capabilities which can overcome aged-related cellular senescence in aged mice which are predisposed to bronchiolar and alveolar senescence as shown by Calhoun and colleagues [47].

Finally, given the relevance of stem cell senescence in the context of IPF, we assessed the regenerative role of hAEC Exo. Early hAEC Exo intervention increased gene expression of *β -catenin*, *BMP4*, *LEF*, and *NFATC1* in BASCs. Notably, human umbilical cord MSC-derived exosomes have also been shown to deliver *Wnt4* to stimulate migration and proliferation of skin cells for wound repair [48]. However, aberrant *Wnt/ β -catenin* has been implicated in IPF and should be further studied to understand the effect of hAEC Exo-mediated *Wnt* signaling.

Proliferation of BASCs has been shown to be dependent on *c-MYC*, which regulates G1 and S phase transitioning during cell cycle and an increase in *β -catenin* is known to initiate transcriptional activation of *c-MYC* and *CNND1* [49]. A study by Dong and colleagues showed that depletion of *c-MYC* in BASCs isolated from mice resulted in inhibition of BASC self-renewal [49]. BASC differentiation into alveolar cells is dependent on *NFATC1* binding to *THBS1* triggered by *BMP4* [50]. Here, we showed that hAEC Exo treatment increased *BMP4* expression in BASCs and increased *NFATC1* and *THBS1* expression in MECs. This suggests that early intervention with hAEC Exo encouraged BASC differentiation by stimulating the recently described *NFATc1/BMP4/THBS1* signaling axis [50].

Late hAEC Exo intervention also increased the number of BASCs, which also showed an increased expression of *β -catenin* and *BMP4*. However, unlike in the early intervention group, hAEC Exo treated animals had MECs that showed increased expression of *FZD6*; a *Wnt* ligand receptor and inhibitor of *GSK β 3*, and *GATA6*, which is expressed in distal lung epithelium and regulates differentiation [51, 52]. This increase in BASC expression of *β -catenin* suggests that hAEC Exo intervention may have encouraged BASC proliferation through increased canonical *Wnt* signaling. In support of this, primary BASCs cultured in the presence of hAEC Exo gave rise to more bronchiolar, alveolar, and bronchioalveolar

colonies. Quantitative PCR analysis showed that colonies cultured with hAEC Exo highly expressed *CC10* and *FoxJ1* indicating that hAEC Exo may help retain the BASCs in their undifferentiated state. This is promising given the current hypothesis that the propensity for developing IPF is ultimately an exhaustion of stem/progenitor cells.

Aside from BASCs, we saw a difference in the percentage between ATI and ATII when compared between young and aged. In the lung, ATI cells account for the majority cells in the alveolar epithelium in comparison to ATII. In response to injury, ATII regenerate the lung through clonal expansion and differentiation into ATI cells. This process is deregulated in diseases such as IPF. In saying so, ATI and ATII expansion and differentiation are also dependent on age, as the literature has shown that aged mice are susceptible to increased ATI and ATII cell loss and delayed ATII recovery. In our study, we showed that in young mice, at day 14 bleomycin challenged mice had percentage of ATII cells, which sat between 15% and 30% while ATI cells were approximately 60% and hAEC Exo treatment increased ATII percentage by twofold while ATI cells were not affected. However, in aged mice the percentage bleomycin challenged resulted in an ATII cell percentage between 4% and 8% while the ATI cells were approximately 60%, suggesting aged related alveolar loss. However, despite this age-related disadvantage, hAEC Exo treatment increased the percentage of ATII cells by twofold and slightly increased the percentage of ATI cells.

CONCLUSION

In summary, this study shows that hAEC Exo can exert potent anti-fibrotic, immunomodulatory, and regenerative properties in the setting of bleomycin induced lung injury. This study paves the way for pharmacological development of cell-derived products that may overcome the hurdles associated with cell-based therapies. Intranasal delivery and ease of long-term storage without the need for liquid nitrogen and the ability to produce exosomes in a cost-effective and scalable manner are some of the advantages of exosome-based therapeutics over cell-based therapies. Furthermore, this multi-modal approach may be more efficacious compared with current drugs such as pirfenidone and nintedanib by addressing the degenerative aspects of IPF and similar diseases. This is the first study describing the anti-fibrotic and pro-regenerative potential of hAEC Exo in the context of lung injury. Future studies should be directed at validating the pathways where miRNA and protein cargo are enriched and optimizing cell conditions to obtain the most potent exosomes for this application.

AUTHOR CONTRIBUTIONS

J.L.T.: designed, performed experiments, analyzed data, prepared and edited the manuscript. S.N.L. and S.T.C.: performed experiments and analyzed data. B.L., M.I.S., and D.D.Z.: were responsible for immunohistochemistry and immunofluorescence experiments. M.K., H.N., and L.S.: contributed to exosome content including imaging and manuscript preparation. C.K.: contributed her expertise with BASC isolation, culture, analyses, and manuscript preparation. W.S. and E.M.W.: analyzed data and contributed to manuscript preparation. R.L.: designed and performed experiments, analyzed data, prepared and edited the manuscript. J.L.T and R.L. Contributed to final approval of the manuscript.

DISCLOSURE OF POTENTIAL CONFLICTS OF INTEREST

E.M.W. is named inventor on patents for the application of amnion cells in lung diseases and amnion exosomes as a regenerative therapy. R.L. has intellectual property rights with Regenasome Pty Ltd., has a consultant/advisory role with Meluha Capital, and has research funding from United Therapeutics. The other authors indicated no potential conflicts of interest.

NOTE ADDED IN PROOF

This article was published online on 3 January 2018. Minor style edits have been made that do not affect data. This notice is included in the online and print versions to indicate that both have been corrected 29 January 2018.

REFERENCES

- Raghu G, Collard HR, Egan JJ et al. An official ATS/ERS/JRS/ALAT statement: Idiopathic pulmonary fibrosis: Evidence-based guidelines for diagnosis and management. *Am J Respir Crit Care Med* 2012;183:788–824.
- Behr J, Kreuter M, Hoepfer MM et al. Management of patients with idiopathic pulmonary fibrosis in clinical practice: The INSIGHTS-IPF registry. *Eur Respir J* 2015;46:186–196.
- Azuma A, Nukiwa T, Tsuboi E et al. Double-blind, placebo-controlled trial of pirfenidone in patients with idiopathic pulmonary fibrosis. *Am J Respir Crit Care Med* 2005;171:1040–1047.
- Alder JK, Cogan JD, Brown AF et al. Ancestral mutation in telomerase causes defects in repeat addition processivity and manifests as familial pulmonary fibrosis. *PLoS Genet* 2011;7:e1001352.
- Chambers DC, Hopkins PMA. Idiopathic pulmonary fibrosis: A degenerative disease requiring a regenerative approach. *Am J Respir Crit Care Med* 2013;188:252–253.
- Li X, Wang Y, An G et al. Bone marrow mesenchymal stem cells attenuate silica-induced pulmonary fibrosis via paracrine mechanisms. *Toxicol Lett* 2017;270:96–107.
- Li X, An G, Wang Y et al. Anti-fibrotic effects of bone morphogenetic protein-7-modified bone marrow mesenchymal stem cells on silica-induced pulmonary fibrosis. *Exp Mol Pathol* 2017;102:70–77.
- Lan Y-W, Theng S-M, Huang T-T et al. Oncostatin M-preconditioned mesenchymal stem cells alleviate bleomycin-induced pulmonary fibrosis through paracrine effects of the hepatocyte growth factor. *STEM CELLS TRANSLATIONAL MEDICINE* 2017;6:1006–1017.
- Reddy M, Fonseca L, Gowda S et al. human adipose-derived mesenchymal stem cells attenuate early stage of bleomycin induced pulmonary fibrosis: Comparison with pirfenidone. *Int J Stem Cells* 2016;9:192–206.
- Uji M, Nakada A, Nakamura T et al. Effect of intratracheal administration of adipose-derived stromal cells on bleomycin-induced lung injury in a rat model. *Osaka City Med J* 2015;61:81–91.
- Cargnoni A, Gibelli L, Tosini A et al. Transplantation of allogeneic and xenogeneic placenta-derived cells reduces bleomycin-induced lung fibrosis. *Cell Transplant* 2009;18:405–422.
- Wei L, Zhang J, Yang Z-L et al. Extracellular superoxide dismutase increased the therapeutic potential of human mesenchymal stromal cells in radiation pulmonary fibrosis. *Cytotherapy* 2017;19:586–602.
- Min F, Gao F, Li Q et al. Therapeutic effect of human umbilical cord mesenchymal stem cells modified by angiotensin-converting enzyme 2 gene on bleomycin-induced lung fibrosis injury. *Mol Med Report* 2015;11:2387–2396.
- Glassberg MK, Minkiewicz J, Toonkel RL et al. Allogeneic human mesenchymal stem cells in patients with idiopathic pulmonary fibrosis via intravenous delivery (AETHER): A phase I, safety, clinical trial. *Chest* 2016;151:971–981.
- Chambers DC, Enever D, Ilic N et al. A phase 1b study of placenta-derived mesenchymal stromal cells in patients with idiopathic pulmonary fibrosis. *Respirology* 2014;19:1013–1018. 1
- Pathan A, Farid T, Khan AR et al. Abstract 34: Human cardiac mesenchymal cell derived extracellular vesicles promote angiogenesis through angiopoietin-TIE2 Signaling. [Abstract] signaling. *Circ Res* 2016;119:A34.
- Shentu TP, Wong S, Espinoza C et al. Extracellular vesicles isolated from human mesenchymal stem cells promote resolution of pulmonary fibrosis. *FASEB J* 2016;130:160.2.
- Leoni G, Neumann P-A, Kamaly N et al. Annexin A1-containing extracellular vesicles and polymeric nanoparticles promote epithelial wound repair. *J Clin Invest* 2015;125:1215–1227.
- Zhao B, Zhang Y, Han S et al. Exosomes derived from human amniotic epithelial cells accelerate wound healing and inhibit scar formation. *J Mol Histol* 2017;48:121–132.
- Heijnen HF, Schiel AE, Fijnheer R et al. Activated platelets release two types of membrane vesicles: Microvesicles by surface shedding and exosomes derived from exocytosis of multivesicular bodies and alpha-granules. *Blood* 1999;94:3791–3799.
- Van Niel G, Raposo G, Candalh C et al. Intestinal epithelial cells secrete exosome-like vesicles. *Gastroenterology* 2001;121:337–349.
- Wolffers J, Lozier A, Raposo G et al. Tumor-derived exosomes are a source of shared tumor rejection antigens for CTL cross-priming. *Nat Med* 2001;7:297–303.
- Zhang B, Yin Y, Lai RC et al. Immunotherapeutic potential of extracellular vesicles. *Front Immunol* 2014;5:518.
- Hyun J, Wang S, Kim J et al. MicroRNA125b-mediated Hedgehog signaling influences liver regeneration by chorionic plate-derived mesenchymal stem cells. *Sci Rep* 2015;5:14135.
- Murphy SV, Kidoor A, Reid T et al. Isolation, cryopreservation and culture of human amnion epithelial cells for clinical applications. *J Vis Exp* 2014;94.
- Murphy S, Rosli S, Acharya R et al. Amnion epithelial cell isolation and characterization for clinical use. *Curr Protoc Stem Cell Biol*; 2010;1:1E.6.
- Moodley Y, Ilancheran S, Samuel C et al. Human amnion epithelial cell transplantation abrogates lung fibrosis and augments repair. *Am J Respir Crit Care Med* 2010;182:643–651.
- Murphy S, Lim R, Dickinson H et al. Human amnion epithelial cells prevent bleomycin-induced lung injury and preserve lung function. *Cell Transplant* 2011;20:909–923.
- Lötvall J, Hill AF, Hochberg F et al. Minimal experimental requirements for definition of extracellular vesicles and their functions: A position statement from the International Society for Extracellular Vesicles. *J Extracell Vesicles* 2017;3:26913.
- Chamoto K, Gibney BC, Lee GS et al. Migration of CD11b+ accessory cells during murine lung regeneration. *Stem Cell Res Ther* 2013;10:267–277.
- Wynn TA. Cellular and molecular mechanisms of fibrosis. *J Pathol* 2008;214:199–210.
- Hodge A, Lourenz D, Vaghjiani V et al. Soluble factors derived from human amniotic epithelial cells suppress collagen production in human hepatic stellate cells. *Cytotherapy* 2014;6:1132–1144.
- Cargnoni A, Piccinelli EC, Ressel L et al. Conditioned medium from amniotic membrane-derived cells prevents lung fibrosis and preserves blood gas exchanges in bleomycin-injured mice-specificity of the effects and insights into possible mechanisms. *Cytotherapy* 2014;16:17–32.
- Liu Y, Martinez L, Ebine K et al. Role for mitogen-activated protein kinase p38 α in lung epithelial branching morphogenesis. *Dev Biol* 2008;314:224–235.
- Vergadi E, Ieronymaki E, Lyroni K et al. Akt signaling pathway in macrophage activation and M1/M2 polarization. *J Immunol* 2017;198:1006–1014.
- Zhang W, Xu W, Xiong S. Macrophage differentiation and polarization via phosphatidylinositol 3-kinase/Akt-ERK signaling pathway conferred by serum amyloid P component. *J Immunol* 2011;187:1764–1777.
- Borensztajn K, Crestani B, Kolb M. Idiopathic pulmonary fibrosis: From epithelial injury to biomarkers—insights from the bench side. *Respiration* 2013;86:441–452.
- Kim SH, Kim S, Oligino TJ et al. Effective treatment of established mouse collagen-induced arthritis by systemic administration of dendritic cells genetically modified to express FasL. *Mol Ther* 2002;6:584–590.

39 Cui H, Banerjee S, Xie N et al. MicroRNA-27a-3p is a negative regulator of lung fibrosis by targeting myofibroblast differentiation. *Am J Respir Cell Mol Biol* 2016;54:843–852.

40 Fang S, Xu C, Zhang Y et al. Umbilical cord-derived mesenchymal stem cell-derived exosomal micRNAs suppress myofibroblast differentiation by inhibiting the transforming growth factor- β /SMAD2 pathway during wound healing. *STEM CELLS TRANSLATIONAL MEDICINE* 2016;5:1425–1439.

41 Hu H, Xu Z, Li C et al. MiR-145 and miR-203 represses TGF- β -induced epithelial-mesenchymal transition and invasion by inhibiting SMAD3 in non-small cell lung cancer cells. *Lung Cancer* 2016;97:87–94.

42 Cui H, Ge J, Xie N et al. miR-34a inhibits lung fibrosis by inducing lung fibroblast senescence. *Am J Respir Cell Mol Biol* 2017;56:168–178.

43 Venugopal SK, Jiang J, Kim T-H et al. Liver fibrosis causes downregulation of miRNA-150 and miRNA-194 in hepatic stellate cells, and their overexpression causes decreased stellate cell activation. *Am J Physiol Gastrointest Liver Physiol* 2010;298:G101–G106.

44 Mahoney JE, Mori M, Szymaniak AD et al. The hippo pathway effector Yap controls patterning and differentiation of airway epithelial progenitors. *Dev Cell* 2014;30:137–150.

45 Liu T, Ullenbruch M, Young Choi Y et al. Telomerase and telomere length in pulmonary fibrosis. *Am J Respir Cell Mol Biol* 2013;49:260–268.

46 Alder JK, Barkauskas CE, Limjunyawong N et al. Telomere dysfunction causes alveolar stem cell failure. *Proc Natl Acad Sci USA* 2015; 112:5099–5104.

47 Calhoun C, Shivshankar P, Saker M et al. Senescent cells contribute to the physiological

remodeling of aged lungs. *J Gerontol A Biol Sci Med Sci* 2016;71:153–160.

48 Zhang B, Wu X, Zhang X et al. Human umbilical cord mesenchymal stem cell exosomes enhance angiogenesis through the Wnt4/ β -catenin pathway. *STEM CELLS TRANSLATIONAL MEDICINE* 2015;4:513–522.

49 Dong J, Sutor S, Jiang G et al. c-Myc regulates self-renewal in bronchoalveolar stem cells. *PLoS One* 2011;6:e23707.

50 Lee J-H, Bhang DH, Beede A et al. Lung stem cell differentiation in mice directed by endothelial cells via a BMP4-NFATc1-thrombospondin-1 axis. *Cell* 2014;156:440–455.

51 Yang H, Lu MM, Zhang L et al. GATA6 regulates differentiation of distal lung epithelium. *Development* 2002;129:2233–2246.

52 Bruno MD, Korfhagen TR, Liu C et al. GATA-6 activates transcription of surfactant protein A. *J Biol Chem* 2000;275:1043–1049.



See www.StemCellsTM.com for supporting information available online.